TISSUE ENGINEERING: Part A
Volume 00, Number 00, 2010

DOI: 10.1089/ten.tea.2009.0343

Original Article

Reversine Enhances Generation of Progenitor-Like Cells by Dedifferentiation of Annulus Fibrosus Cells

Mansi Saraiya, B.S.,[1] Rena Nasser, M.D.,[1] Yan Zeng, M.D.,[1,2] Sankar Addya, Ph.D.,[3] Ravi Kumar Ponnappan, M.D.,[1] Paolo Fortina, M.D., Ph.D.,[3] David Greg Anderson, M.D.,[1] Todd J. Albert, M.D.,[1] Irving M. Shapiro, Ph.D.,[1] and Makarand V. Risbud, Ph.D.[1]

The aim of this study was to determine if treatment with reversine, a purine analog, promoted generation of skeletal progenitor cells from lineage-committed annulus fibrosus cells. Reversine modulated cell growth, morphology, and the actin cytoskeleton of annulus fibrosus cells. Microarray profiling coupled with Ingenuity Pathway Analysis revealed that reversine treatment resulted in a significant expression change in many genes including those required for cell–cell interaction, cell movement, cell growth, and development. Further analysis revealed that there was involvement of gene networks concerned with cellular assembly and organization, DNA replication and repair, tissue morphology, and cell-to-cell signaling. The gene expression profile was dependent on reversine concentration. In osteogenic media, cells pretreated with 300 nM reversine exhibited an increased induction in alkaline phosphatase activity and enhanced expression of alkaline phosphatase, bone sialoprotein, osteocalcin, and collagen type I mRNA. Maintained in adipogenic media, the reversine-pretreated annulus cells displayed evidence of adipogenic differentiation: accumulation of cytosolic lipid droplets and increased expression of PPAR-γ2, LPL, and Fabp mRNA. In chondrogenic media, cells pretreated with reversine exhibited marked increase in the induction of aggrecan, collagen types II, IX, and XI, and versican. It is concluded that reversine treatment induced annulus fibrosus cell plasticity and promoted their differentiation along mesenchymal lineages. This agent could be used to generate skeletal progenitor cells to orchestrate the repair of the intervertebral disc.

Introduction

The intervertebral disc is a specialized biomechanical structure comprising a highly hydrated central nucleus pulposus surrounded by a ligamentous annulus fibrosus. A layer of cartilage, the endplate, separates the disc from vertebral bone. Changes in applied biomechanical forces and slow diffusion of nutrients and oxygen delivery across the endplate are seen as major causes of degenerative disc disease.[1,2]

Within the past decade, there has been a growing interest in developing strategies to repopulate the degenerated intervertebral disc using embryonic as well as adult mesenchymal stem cells (MSCs).[3–5] It has been shown that these transplanted cells can be used to regenerate the nucleus pulposus and partially restore function.[6,7] A major shortfall of cell transplantation therapies using autologous adult stem cells derived from the marrow, fat, or other tissue sources is that the cells are not committed/adapted to the unique microenvironmental conditions of the degenerating disc.[8] One implication of this lack of environmental conditioning is that there is a loss of cells following transplantation, and usually functional restoration is far from complete.[9] Recently, a more direct approach using the resident progenitor cells to repopulate the damaged tissue has been proposed.[10] Although interesting, this approach is limited because of deficits in understanding of factors that control the commitment of endogenous disc progenitor cells.

An alternate strategy to offset the limited capacity for self-renewal is to generate multipotent progenitors from adult differentiated cells. Recently, a substituted purine, reversine, has been used to induce reversion of adult cells to a multipotent state; under appropriate conditions, these cells could then be converted into other cell types.[11,12] Based on these findings, we explored the possibility that reversine treatment can be used to reprogram lineage-committed annulus fibrosus cells to a stem-like state. The results of this study indicate that annulus fibrosus cells can be dedifferentiated into progenitor cells, which can then be committed to chondrogenic, osteogenic, or adipogenic lineages. Based on these results, we advance the notion that it may be possible

[1]Department of Orthopaedic Surgery and Graduate Program in Tissue Engineering and Regenerative Medicine, Thomas Jefferson University, Philadelphia, Pennsylvania.
[2]Department of Orthopaedic Surgery, Peking University Third Hospital, Beijing, P.R. China.
[3]Department of Cancer Biology, Kimmel Cancer Center, Thomas Jefferson University, Philadelphia, Pennsylvania.

to use reversine to generate progenitor cells to repair the degenerated disc.

Materials and Methods

Cell isolation

We used an explant culture technique to isolate annulus fibrosus cells from the intervertebral discs of mature Wistar rats.[13] Annulus fibrosus tissue pooled from three to four rats per isolation was partially digested by treatment with 60 U/mL collagenase (Sigma, St. Louis, MO) and 10 U/mL hyaluronidase (Sigma) for 3–5 h in spinner flasks fitted with magnetic stirrers. The partially digested tissue, along with liberated cells, was cultured as an explant in Dulbecco's modified Eagle's medium and 10% fetal bovine serum supplemented with antibiotics (Gibco, Grand Island, NY) in a humidified atmosphere containing 5% CO_2 at 37°C. Adherent fibroblastic cells exhibiting an elongated morphology migrated out of the explant after 1 week. These cells express high levels of collagen type I and fibromodulin, markers of the annulus fibrosus phenotype.

Reversine treatment

Annulus fibrosus cells (passages 1 and 2) plated at a density of 12,000 cells/cm^2 were treated with reversine (50 nM to 20 μM) for 1–4 days, and cell growth and morphology were assessed. For microarray analysis and differentiation assays, cells were treated with 300 nM and 5 mM reversine for 4 days prior to RNA isolation or induction with differentiation media.

Measurement of cell viability and growth

To measure cell viability, MTT (3-(4,5-dimethylthiazol-2-yl)-2,5-diphenyltetrazolium bromide) assay was carried out as described previously.[14] Briefly, after reversine treatment, MTT diluted in Hank's balanced salt solution was added to the culture medium to a final concentration of 0.5 mg/mL. At the end of the incubation period (2 h at 37°C), the medium was removed, and the precipitated formazan crystals were solubilized in dimethyl sulfoxide. Product formation was measured by reading the absorbance at 560 nm using a microplate reader (Spectra Flour Plus; Tecan, Durham, NC).

Assessment of cell morphology and actin organization

Crystal violet staining was used to monitor the morphology of cells treated with reversine for various time periods. Images were captured using a bright-field microscope fitted with a digital camera (Nikon, Melville, NY). To observe actin organization, cells were plated in 96-well plates (4×10^4 cells/well). After reversine treatment, cells were fixed with 4% paraformaldehyde, permeabilized 0.1% Triton X-100 for 5 min, and labeled with 488 Phalloidin (Invitrogen, Carlsbad, CA) for 30 min. Cells were washed with phosphate-buffered saline (PBS) and visualized using a confocal microscope (Olympus Fluoview; Olympus, Tokyo, Japan).

Analysis of cell surface marker expression by flow cytometry

Annulus fibrosus cells were treated with reversine (300 nM) for 4 days and analyzed for the expression of cell surface receptors. They were detached from the tissue culture plates using a nonenzymatic digestion solution and washed twice with PBS. Cells were then suspended in PBS supplemented with 5% fetal calf serum and treated with the following monoclonal antibodies for expression of known stem cell markers: CD90, CD29 (integrin β1), CD44 (hyaluronate receptor), and CD45 (all from BD Pharmingen, San Jose, CA). In each case, a two-colored antibody labeling procedure was employed: CD90-phycoerythrin (PE)/CD29-fluorescein isothiocyanate (FITC). After 1 h at 37°C, cells were washed twice with PBS and subjected to flow cytometry using a Beckman Coulter XL system (Beckman, Miami, FL) equipped with a 488 argon ion laser and a four-color detector.

Microarray analysis

Total RNA was isolated from untreated annulus fibrosus cells and from the cells that were treated with reversine (300 nM and 5 mM) for 4 days using RNAeasy mini columns (Qiagen, Valencia, CA). Before elution from the column, RNA was treated with RNase-free DNAse I. RNA was quantified on a Nanodrop ND-100 spectrophotometer (NanoDrop Technologies, Wilmington, DE), followed by RNA quality assessment by analysis on an Agilent 2100 bioanalyzer (Agilent, Palo Alto, CA). RNA amplification and labeling were performed by the WT-Ovation Pico RNA amplification system (NuGen Technologies, San Carlos, CA). Briefly, 50 ng of total RNA was reverse transcribed using a chimeric cDNA/mRNA primer, and a second complementary cDNA strand was synthesized. Purified cDNA was then amplified with ribo-SPIA enzyme and SPIA DNA/RNA primers (NuGen Technologies). Amplified DNA was purified with Zymo Research DNA Clean and Concentrator-25 (Zymo Research, Orange, CA). Sense transcript cDNA (ST-cDNA) was generated from 3 μg amplified cDNA using WT-Ovation Exon module (NuGen Technologies). Purified ST-cDNA was assessed for yield using the Nanodrop spectrophotometer (NanoDrop Technologies). Five micrograms of ST-cDNA was fragmented and chemically labeled with biotin to generate biotinylated ST-cDNA using FL-Ovation cDNA biotin module V2 (NuGen Technologies).

Each Affymetrix gene chip rat gene 1.0 ST array (Affymetrix, Santa Clara, CA) was hybridized with fragmented and biotin-labeled target (4.5 μg) in 200 μL of hybridization cocktail. Target denaturation was performed at 99°C for 2 min and then 45°C for 5 min, followed by hybridization for 18 h. Then the arrays were washed and stained using Genechip Fluidic Station 450, and hybridization signals were amplified using antibody amplification with goat IgG (Sigma-Aldrich, St. Louis, MO) and antistreptavidin biotinylated antibody (Vector Laboratories, Burlingame, CA). The chips were scanned on an Affymetrix Gene Chip Scanner 3000, using Command Console Software. Background correction and normalization were done using Robust Multichip Average with Genespring V 10.0 software (Agilent). A 1.5-fold differentially expressed gene list was generated. The listing of differentially expressed genes and their *p*-values were loaded into Ingenuity Pathway Analysis (IPA) 5.0 software (www.ingenuity.com) to perform biological network and functional analyses. IPA converts gene sets (with or without expression information) into related molecular networks based on IPA knowledge database. A core analysis was performed for and the genes were categorized based on molecular function, mapped to genetic net-

works, and ranked by score. The score reflects the probability that a collection of genes equal to or greater than a number in the network could not be achieved by chance alone. A score of more than 10 was used as a cutoff for identifying specific gene networks. Independent validation of selected differentially expressed genes was performed using real-time reverse transcriptase–polymerase chain reaction (RT-PCR).

Real-time RT-PCR analysis

Following treatment with reversine or culture in differentiation media, total RNA was extracted from cells using RNAeasy mini columns (Quiagen). Before elution from the column, RNA was treated with RNase-free DNAse I. One-hundred nanograms of total RNA was used as template for real-time PCR analysis. Reactions were set up in microcapillary tubes using 1 μL RNA with 9 μL of LightCycler FastStart DNA Master SYBR Green I mix (Roche Diagnostics, Indianapolis, IN) to which gene-specific forward and reverse PCR primers were added. Each set of samples included a template-free control. PCR reactions were performed in a LightCycler (Roche Diagnostics) according to the manufacturer's instructions. All the primers used were synthesized by Integrated DNA Technologies (Coralville, IA).

Cell differentiation assays

To induce differentiation, the reversine-treated annulus fibrosus cells (passages 1 and 2) were seeded in multiwell plates (5000 cells/cm^2 for osteogenesis and 21,000/cm^2 for adipogenesis), cultured overnight in standard culture medium, and treated with osteogenic or adipogenic supplements. Osteogenic supplements consisted of dexamethasone (10^{-7} M),

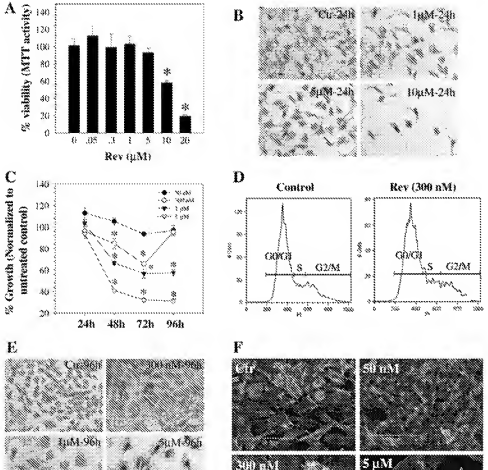

FIG. 1. Viability of annulus fibrosus cells following treatment with reversine (50 nM to 20 μM). (**A**) Cell viability measured using the MTT assay after 24 h. At 10 and 20 μM reversine, the annulus cells displayed a marked decrease in viability. (**B**) Morphology of reversine-treated annulus fibrosus cells after 24 h. At 10 μM, very few cells remained attached to the tissue culture dish. Magnification: ×20. (**C**) Effects of reversine concentration on annulus fibrosus cell number. Annulus cells were treated with reversine (50 nM to 5 μM) for time periods up to 96 h and cell number was measured using the MTT assay. Note that above 50 nM, there was a profound decrease in cell proliferation. Values shown are expressed as a function of the number of untreated cells at each time point and concentration. (**D**) Cell cycle analysis of annulus fibrosus cells treated with 300 nM reversine. Reversine-treated cells showed no significant difference in G0/G1 (53.63 + 18.08), S (22.72 + 13.41), and G2M (16.25 + 3.88) phases compared with untreated controls (G0/G1: 72.69 + 22.71; S: 15.41 + 13.83; G2M: 9.06 + 6.04) after 4 days. There was no difference in the number of apoptotic cells (treated: 7.8 + 4.7; untreated: 3.3 + 3.74). (**E**) Morphology of cells at 96 h after reversine treatment. Concentrations of reversine above 1 μM caused hypertrophy of the annulus fibrosus cells. Magnification: ×20. (**F**) Actin cytoskeletal organization of annulus fibrosus cells treated with reversine and stained with phalloidin. Above 300 nM reversine, there was a significant alteration in organization and orientation of actin filaments. Results are the mean + SD of three independent experiments; $^*p < 0.05$. MTT, 3-(4,5-dimethylthiazol-2-yl)-2,5-diphenyltetrazolium bromide; SD, standard deviation.

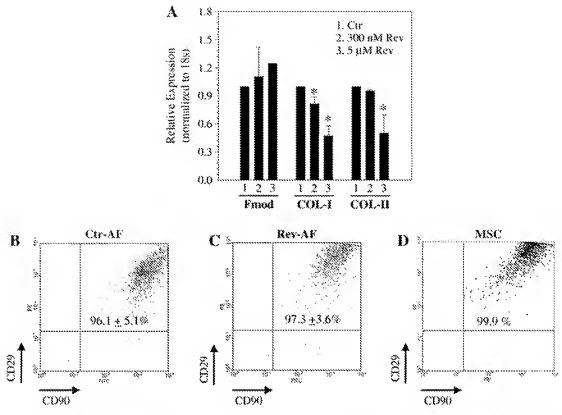

FIG. 2. Phenotypic assessment of reversine-treated annulus fibrosus cells. (A) Cells show decreased expression of collagen type I (COL-I) after reversine treatment; decrease in collagen type II (COL-II) was evident only at 5 μM reversine. Fibromodulin (Fmod) showed no change. (**B–D**) Effect of reversine on cell surface marker expression. Cells were colabeled with CD29 and CD90 and analyzed by flow cytometry. Rat bone marrow MSCs were used as a positive control. There was no significant difference in expression of both these surface markers by reversine treatment (Rev-AF) when compared with untreated annulus fibrosus cells (Ctr-AF). Results are the mean ± SD of three independent experiments; $^{*}p < 0.05$. MSCs, mesenchymal stem cells; FITC, fluorescein isothiocyanate; PE, phycoerythrin.

ascorbate 2-phosphate (50 μg/mL), and β-glycerophosphate (10^{-2} M).[18] Adipogenic supplements included dexamethasone (10^{-6} M), insulin (1 μg/mL), 1-methyl-3-isobutylxanthine (5×10^{-4} M), and indomethacin (10^{-4} M).[16,17] For adipogenic differentiation, fetal bovine serum was replaced with rabbit serum to enhance adipogenic differentiation.[17] Cells were treated with osteogenic supplements for 9 or 16 days, whereas with adipogenic supplements in multiple cycles of 3 days, followed by 24 h recovery in growth medium supplemented with insulin. For differentiation into the chondrogenic phenotype, cells were encapsulated in 1.2% alginate (LVG; Pronova, Lysaker, Norway) (1×10^{6} cells/mL of alginate) in high-glucose Dulbecco's modified Eagle's medium supplemented with insulin–transferin–selenium (with albumin), sodium pyruvate (100 μg/mL), L-proline (40 μg/mL), ascorbate 2-phosphate (50 μg/mL), and transforming growth factor β3 (10 ng/mL) for 21 days.[16]

Histochemical staining of differentiating cells

Alkaline phosphatase localization. After 9 days in culture in osteogenic medium, cells were fixed in 2% formaldehyde in methanol and stained with naphthol As-Bi-phosphate solution in sodium nitrite (0.1 M) and FBB-alkaline solution for 30 min at 37°C in the dark.

Oil red-O staining. To localize lipid droplets, cells were stained with oil red-O as described previously.[16,17] Cells were washed with PBS and fixed for 30 min in phosphate-buffered 3.7% formaldehyde. After washing with water and then 60% isopropanol, the cells were stained with 0.3% oil red-O in 60% isopropanol for 1 h at room temperature. The cultures were then extensively washed with water to remove excess stain and then observed with an inverted phase contrast microscope.

Statistical analysis

Data are presented as mean ± standard deviation. To test for significance, data were analyzed using Student's *t*-test; the obtained *p*-values are indicated in the text and figures.

Results

Figure 1A shows the viability of annulus fibrosus cells treated with reversine for 24 h. At 0.05–5.0 μM reversine, there was no significant difference in viability between treated and untreated cells. At higher concentrations (10 and 20 μM), there was a significant decrease in cell viability. Microscopic observation of the treated cells indicates that there was a dramatic reduction in number of adherent cells at a dose of 10 μM and above; in contrast, at reversine con-

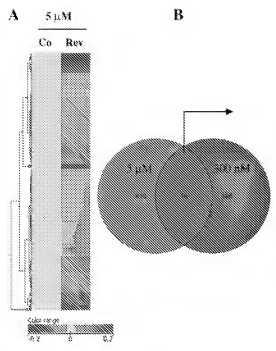

Gene Bank #	Gene Symbol	Fold Co/Rev 300 nM	Fold Co/Rev 5 μM
BC087003	Dusp6	1.92	0.5
D14437	Cnn1	1.90	0.4
BC078865	Hsd11b1	1.88	0.59
M83745	Pcsk1	0.60	0.61
M24067	Serpine1	1.56	0.27
BC060537	Tnfrsf12a	1.54	0.36
BC072544	Ppap2b	1.54	3.9

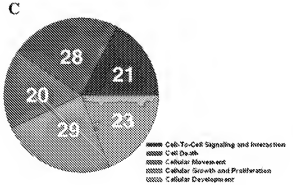

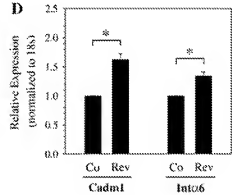

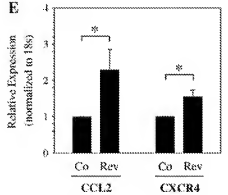

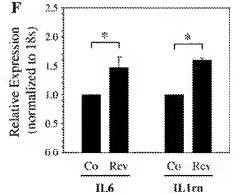

FIG. 3. Effect of reversine treatment on annulus fibrosus gene expression. (**A**) Microarray analysis of cells treated with 5 μM reversine (Rev) for 96 h. The heat map shows the differential expression of 426 genes after reversine treatment (**B**) Venn diagram showing subset of genes that were affected by either 300 nM or 5 μM reversine. List of a number of common genes that were modulated at both 300 nM or 5 μM of reversine is shown. In almost every case, except Ppap2b, at the higher reversine concentration, there was a decrease in expression of these genes. (**C**) Pie chart showing differentially expressed genes based on major molecular and cellular functions. The number represents genes associated with a specific function. Note that some genes may have multiple functions and can be classified in several categories (see Table 1 for details). (**D–F**) Changes in levels of expressed genes verified by real-time RT-PCR analysis. Reversine treatment (300 nM) increased expression of (**D**) cell adhesion molecule 1 (Cadm1) and integrin α6 (Itgb6), (**E**) CCL2 and CXCR4, and (**F**) IL6 and IL1 receptor antagonist (IL1rn) compared with untreated control cells. $n = 3$; mean + SD; $^*p < 0.05$. Co, control; RT-PCR, reverse transcriptase–polymerase chain reaction. Color images available online at www.liebertonline.com/ten.

Table 1. Genes Modulated by Reversine Grouped According to Cellular and Molecular Functions

No.	Molecular functions	No. of molecules	p-Value	Gene symbol
1	Cell-to-cell signaling and interaction	21	2.41 E − 07 to 5.79 E − 03	CD55, ARHGDIB, CADM1, CCL13, CXCR4, CYR61, EDN, GFRA1, IL6, ITGA3, ITGA6, PCDHB6, PPAP2B, SERPINE1, TNFRSF12A, VCAN, TLR3, PCSK1, TNFSF18, IL1RN
2	Cell death	28	4.75 E − 07 to 4.24 E − 03	BTG2, CADM1, CCL3, CD55, CKAP2, CXCR4, CYR61, DUSP6, EDN1, FST, GFRA1, IL6, IL1RN, ITGA6, NQO1, PAX7, PLK2, PTGS1, RNASE1, SERPINE1, SGMS2, TNFSF18, VCAN, NTLR3, TNFRSF12A, E1, GRM3, AKAP13
3	Cellular movement	20	1.47 E − 06 to 4.70 E − 03	ARHGDIB, CCL13, CD55, CXCR4, CYR61, DNAJB4, EDN1, GFRA1, IL6, IL1RN, ITGA3, ITGA6, SERPINE1, TLR3, TNFRSF12A, VCAN, ACAN, CADM1, CNN1, PPAP2B
4	Cellular growth and proliferation	29	1.66 E − 06 to 5.79 E − 03	AKAP13, BTG2, CADM1, CCL13, CNN1, CXCR4, CYR61, DNAJB4, EDN1, FST, HSD11B1, IL6, IL1RN, ITGA3, ITGA6, MTBP, PTGS1, SERPINE1, TLR3, TNFRSF12A, TNFSF18, TPX2, UCHL1, VCAN, GFRA1, CD55, DUSP6, PLK2, PAX7
5	Cellular development	23	4.68 E − 06–5.70 E − 03	ACAN, AKAP13, CADM1, CCL13, CXCR4, CYR61, EDN1, FST, GFRA1, IL6, IL1RN, ITGA3, ITGA6,, PAX7, TLR3, VCAN, ZNF488, TNFRSF12A, BTG2, CD55, RNASE1, PLK2, HSD11B1

centration up to 5 μM, cells remain healthy and maintain their normal morphology (Fig. 1B). When compared with untreated cells, at reversine concentrations greater than 50 nM, there was a marked decrease in cell proliferation without inducing cell toxicity for periods of time up to 96 h (Fig. 1C). At 96 h, recovery of 300 nM reversine-treated cells was comparable to the untreated control. Flow cytometric analysis was performed to further confirm this finding. Figure 1D shows that both control and cells treated with reversine (300 nM) after 4 days exhibit no significant difference in the percentage of cells present in different phases of the cell cycle. We examined the effect of reversine treatment on size and morphology of the annulus fibrosus cells after 48–96 h of treatment. At concentrations above 300 nM, reversine affects both cell size and shape. Figure 1E, F shows that the treated cells were hypertrophic and acquire a flattened, epithelial-like morphology. We used phalloidin labeling to monitor actin stress fiber distribution and organization (Fig. 1F). Again, above 300 nM, the hypertrophic annulus fibrosus cells displayed a marked alteration in phalloidin staining, suggesting altered actin organization.

Figure 2A depicts expression of annulus fibrosus genes after reversine treatment. Expression of collagen type-I was decreased following 300 nM and 5 μM reversine treatment, whereas collagen type-II was suppressed only at 5 μM. Fibromodulin expression was unaffected by reversine. We then immunophenotyped annulus fibrosus cells treated with reversine (300 nM) for 4 days by flow cytometry. A high percentage of reversine-treated annulus fibrosus cells and MSCs expressed CD90, CD29, as well as CD44 (control: 99.85% ± 0.21%; reversine treated: 99.09% ± 1.28%; MSCs: 100%; Fig. 2B–D). The untreated (Fig. 2B) and reversine-treated annulus fibrosus cells (Fig. 2C) displayed no significant change in expression of these markers. We noted that the reversine effects are reversible. With withdrawal of reversine the pretreated annulus fibrosus cells returned to their original size and morphology and the expression of collagens types I and II was restored (not shown).

We performed microarray analysis of annulus fibrosus cells treated with 300 nM and 5 mM reversine for 96 h. Figure 3 shows heat map representing gene expression profile changes following reversine treatment. At 300 nM, reversine treatment changes the expression of 121 genes; when the annulus cells were treated with 5 μM reversine, 426 genes showed a change in expression (Fig. 3A, B). A small subset of genes was modulated at both 300 nM and 5 μM reversine. Figure 3B provides a list of genes that were affected positively or negatively by high and low concentrations of

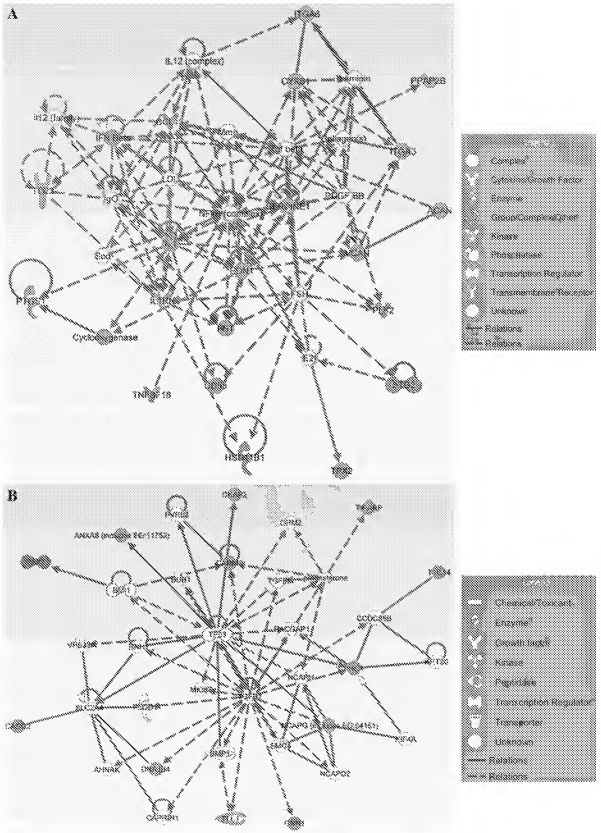

FIG. 4. Functional gene networks identified using IPA from differentially expressed genes between control and 300 nM reversine-treated annulus fibrosus cells. (**A**) Cellular assembly and organization and nutritional disease gene (score 41); (**B**) DNA replication, recombination, and repair, cancer, and cell death network (score 22). Nodes represent genes, whereas shapes represent a functional class of gene product. Intensity of the node color indicates degree of overexpression (red) and the degree of downregulation (green). Genes in uncolored nodes were not identified as differentially expressed and were integrated into computationally generated networks based on information in the IPA database. IPA, Ingenuity Pathway Analysis. Color images available online at www.liebertonline.com/ten.

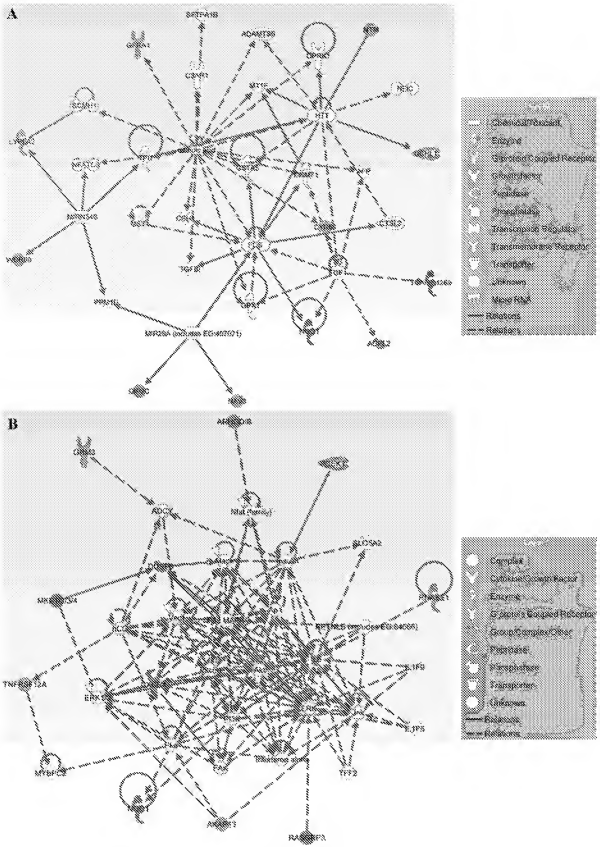

FIG. 5. Functional gene networks identified using IPA for reversine-treated annulus fibrosus cells. (**A**) Tissue morphology, cell-to-cell signaling, and interaction (score 21); (**B**) amino acid metabolism, molecular transport, and small molecular biochemistry (score 19). Colored nodes represent focus genes, whereas genes in uncolored nodes were not identified as differentially expressed and were integrated into networks based on information in the IPA database. Node color indicates degree of overexpression (red) and the degree of downregulation (green). Color images available online at www.liebertonline.com/ten.

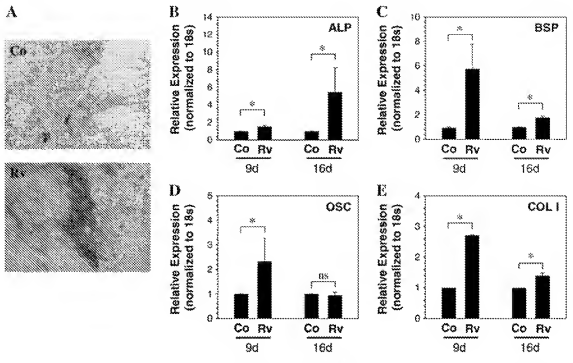

FIG. 6. Osteogenic differentiation of annulus fibrosus cells pretreated with 300 nM reversine. (**A, B**) Alkaline phosphatase (ALP) activity and expression by differentiating cells. Following treatment with reversine (Rv), cells were cultured in osteogenic media for 16 days. The cells were stained for alkaline phosphatase activity or used for real-time RT-PCR analysis. Note the increase in alkaline phosphatase staining compared with control (Co). Magnification: ×20. There was also a significant elevation in alkaline phosphatase transcript level. (**C–E**) Analysis of osteoblast marker gene expression. In cultures treated with osteogenic supplements for 9 and 16 days, reversine-pretreated annulus fibrosus cells exhibited a significant increase in (**C**) bone sialoprotein (BSP), (**D**) osteocalcin (OSC), and (**E**) collagen type I (COL1) mRNA expression at 9 days compared with control cells. $^{*}p < 0.05$; data represent mean ± SD of three independent experiments.

reversine, respectively. The subsequent studies were performed with low concentration of the drug (300 nM). To define the functional properties of the genes that were modulated by reversine treatment, genes were subjected to IPA network and functional and pathway analyses. These analyses indicate that a number of genes related to cell-to-cell signaling, cellular movement, cell growth and proliferation, and cellular and tissue development are modulated by reversine treatment (Fig. 3C). Table 1 provides a complete list of functions, involved genes, and corresponding *p*-values. Expression changes in select genes following treatment with 300 nM reversine were validated by real-time RT-PCR analysis. Note that chemokine ligand 2, interleukin 6, chemokine C-X-C motif receptor 4, microtubule associate protein, and annexin A8 are highly expressed by the reversine-treated cells. Figure 3D shows expression of cell adhesion molecule 1 (Cadm1) and integrin α6 following reversine treatment. A small but significant increase in expression of both Cadm1 and integrin α6 was observed. We also measured mRNA levels of CCL2, CXCR4 (Fig. 3E), IL6, and IL1 receptor antagonist (IL1rn) (Fig. 3F). Again a significant elevation in their expression was seen after reversine treatment. Figures 4 and 5 show the IPA generated networks with scores of 41, 22, 21, and 19. These networks are concerned with cellular assembly and organization (Fig. 4A), DNA replication, recombination, and repair, cell death (Fig. 4B), cell-to-cell signaling, tissue morphology (Fig. 5A), and lastly amino acid metabolism, molecular transport, and small molecular biochemistry (Fig. 5B).

Annulus fibrosus cells pretreated with reversine (300 nM and 5 μM) were cultured under conditions that promote adipogenic, osteogenic, and chondrogenic differentiation. When cultured in an osteogenic medium and stained with naphthol As-Bi-phosphate, an increase in alkaline phosphatase activity is observed in the reversine-pretreated (300 nM) cultures (Fig. 6A); a concomitant induction in alkaline phosphatase mRNA was also seen, which was more pronounced 16 days following treatment (Fig. 6B). In addition, expression of bone sialoprotein, osteocalcin, and collagen type I was induced (Fig. 6C–E). Relative increase in the mRNA levels of these genes was higher at 9 days than at 16 days. There was also evidence of increased mineral deposition in reversine-pretreated cells compared with untreated annulus fibrosus cells after 4 weeks in osteogenic media (not shown). For osteocalcin, after 16 days, there was no significant difference in expression between control and reversine-pretreated cells cultured in the osteogenic medium.

Likewise, when treated with adipogenic supplements for 6 days, oil red-O staining indicated that reversine treatment enhanced lipid droplet formation. After 6 days of treatment, a significantly greater number of reversine-pretreated (300 nM) annulus fibrosus cells contained cytosolic lipid droplets than controls (Fig. 7A). There was an increase in the expression of PPAR-γ2 mRNA, a critical transcription factor involved in adipogenesis after 6 days of treatment (Fig. 7B). Expression of LPL and Fabp mRNA, other important adipocyte marker genes, were also significantly upregulated

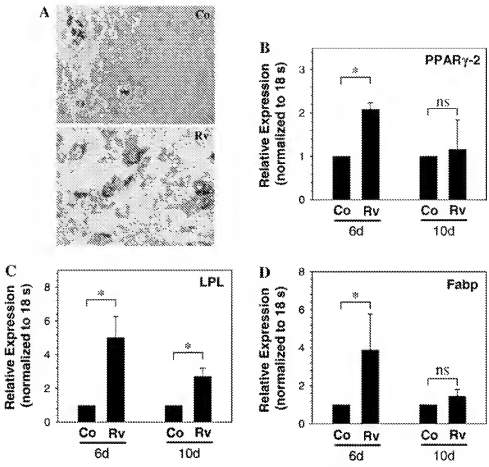

FIG. 7. Adipogenic differentiation of annulus fibrosus cells pretreated with 300 nM reversine. Cells were cultured in adipogenic media for 10 days and histochemical staining and real-time RT-PCR analysis were performed on the differentiating cells. (**A**) Oil red-O staining of control (Co) and reversine (Rv)-pretreated annulus cells after culture in adipogenic media. Reversine-treated cells exhibit increased accumulation of lipid droplets. Magnification: ×20. (**B–D**) Real-time RT-PCR analysis of cells maintained in adipogenic medium. In cultures treated with adipogenic supplements for 6 and 10 days, reversine-pretreated annulus fibrosus cells exhibit significantly increased expression of (**B**) PPAR-γ2, (**C**) LPL, and (**D**) Fabp than control cells. $^{*}p < 0.05$; data represent mean ± SD of three independent experiments.

when compared with controls (Fig. 7C, D). In the absence of differentiating supplements, reversine-pretreated cells did not show transdifferentiation into adipogenic or osteogenic phenotype (not shown). When cultured in conditions that favor chondrogenesis, the reversine-pretreated cells exhibited a significant induction of chondrocytic marker genes including aggrecan (Fig. 8A), collagen type II (Fig. 8B), versican (Fig. 8C), collagen type IX (Fig. 8D), and collagen type XI (Fig. 8E). Related to the effects of different concentrations of reversine, at 5 μM, compared with untreated controls, there were no overt differences in osteogenic and adipogenic differentiation.

Discussion

There are considerable advantages in use of drugs to promote the dedifferentiation of lineage-committed annulus fibrosus cells. Foremost among these is the fact that the somatic annulus cells can be obtained in large numbers and easily harvested. Moreover, although these cells can be committed to a number of lineages, we would reason that the reversine-treated cells may preferentially follow an established differentiation pathway that is relevant to their subsequent use for intervertebral disc repair. In addition, the dedifferentiated annulus cells would not be rejected by the donor, and therefore, epigenetic programming provides a customized approach to transplantation therapy. From this perspective, reversine treatment holds promise of promoting the expression of cells that exhibit MSC-like characteristics. In the hypoxic, hyperosmotic, and mechanically stressed environment of the disc, these cells would reprogram and express phenotypes that could be used to repair or replace annulus cells.

Treatment with very low concentrations of reversine promoted dedifferentiation of the annulus cells. MTT and cell cycle analysis clearly showed that a nanomolar concentration of reversine was nontoxic and well tolerated by the cells. During this period, these cells exhibited a marked decrease in proliferative potential and cell swelling. Indeed, we estimated that the diameter of the dedifferentiated annulus cells was fivefold greater than untreated cells. Although we did not examine the mechanism of cell swelling, other workers have noted that the cells exhibit polyploidy probably due to

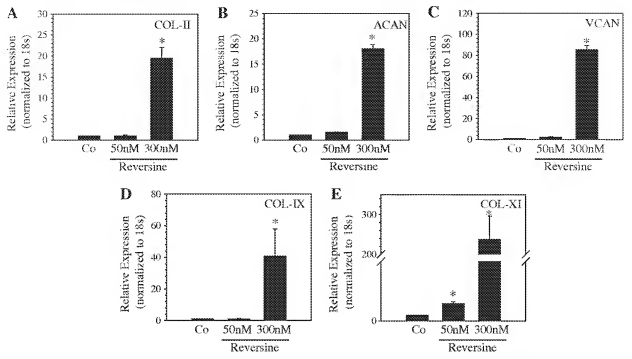

FIG. 8. Chondrogenic differentiation of annulus fibrosus cells pretreated with reversine in alginate beads. RT-PCR analysis of control and reversine-treated (50–300 nM) cells maintained in alginate culture under chondrogenic conditions. Note that there is upregulation in expression of (**A**) collagen type II (COL-II), (**B**) aggrecan (ACAN), (**C**) versican (VCAN), (**D**) collagen type IX, and (**E**) collagen type XI mRNA. Co: untreated cells maintained under chondrogenic conditions. *Significantly different from 50 nM reversine or control (Co); $p < 0.05$; data represent mean + SD of three independent experiments.

reversine-dependent interference with Aurora B kinase activity.[18] This protein kinase has been shown to be required for a number of functions including mitotic chromosome segregation, spindle checkpoint function, cytokinesis, and histone H3 phosphorylation.[19] Sabbattini *et al.* have shown that Aurora B is required to remodel chromatin during post-mitotic cell differentiation of MSCs.[20] Interestingly, our computational network and pathway analysis supported these earlier observations. We determined that reversine treatment affected gene networks that control cellular assembly and organization, DNA replication, recombination, and repair, cell-to-cell signaling, tissue morphology, as well as molecular transport and small molecular biochemistry. This observation strongly suggests that reversine treatment preferentially influences biological functions that include cell-to-cell signaling, cellular movement, and cell growth and proliferation. From this perspective, reversine treatment probably drives annulus fibrosus cells into the dedifferentiated state and the acquisition of MSC-like characteristics through pathways dependent on chromatin remodeling, growth arrest, and cell cycle regulation.

The expression of genes linked to somatic cell dedifferentiation has been discussed in a considerable number of recent studies.[21,22] With respect to reversine treatment, changes in genes linked to dedifferentiated state and the acquisition of an MSC-like phenotype have been documented.[20,23–25] The results of this study have extended these earlier studies by delineating that there is a marked increase in expression of CCL2 and CXCR4, IL-6 and IL-1rn, and Intx6. Of these, the chemokine receptor ligand CCL2 and the receptor CXCR4 have been shown to be present in bone marrow MSCs and serve to support hematopoietic cell proliferation.[26] Likewise, IL-6 protein is secreted by neural stem cells and MSCs and inhibits T-cell proliferation[27]; IL-6 together with IL-3 is required for cell survival and synergistically enhance stem cell recovery.[28] Lastly, there is considerable evidence showing that the Toll-like receptors are expressed on human bone marrow-derived MSCs where they regulate proliferation, differentiation, and expression of the immunosuppressive phenotype.[29,30] Clearly, expression of these receptors would serve to decrease rejection of the dedifferentiated cells as well as promote stem cell plasticity.

The mesengenic potential of the reversine-treated annulus fibrosus cells was evaluated by maintaining the cells in medium that encouraged expression of differentiated phenotypes. In medium supplemented with dexamethasone, ascorbate, and β-glycerophosphate, many more reversine-pretreated cells expressed osteogenic characteristics (high alkaline phosphatase expression and activity and expression of osteogenic proteins) than untreated cells. Likewise, medium containing dexamethasone, insulin, 1-methyl-3-isobutylxanthine, and indomethacin enhanced the expression of PPARγ, LPL, and Fabp; these cells were also positive for oil red-O staining. Importantly, from the perspective of disc regeneration, reversine-pretreated cells showed a significantly enhanced potential to differentiate into chondrocytic cells and expressed high levels of aggrecan, versican, collagen types II, IX, and XI, important matrix constituents of the annulus fibrosus, as well as nucleus pulposus. Moreover, the chondrogenic potential of the reversine-pretreated cells was

many folds greater than the adipogenic or osteogenic potential. This finding lends support to the notion that this agent would be suitable for regenerating the intervertebral disc. Although it was not determined if the reversine-treated cells were multipotent, results of the differentiation assays indicated that annulus fibrosus cells pretreated with reversine exhibited many MSC-like characteristics.[10,16] Accordingly, these findings indicate that reversine reprograms annulus fibrosus cells to a state of increased plasticity so that additional stimuli, such as cell–matrix and cell–cell interactions, may promote differentiation at high frequency.

Currently, it is generally accepted that disc repair can be accomplished through the use of stem cell therapy, but with one exception, all have utilized adult stem cells.[3–7] Of course, the use of these cells for replacement therapy is complicated by problems including limited propagation capacity, restricted differentiation potential, as well as infection at site of harvesting and allograft rejection. Hence, dedifferentiation of adult differentiated cells into multipotent progenitors provides a very attractive clinical procedure for disc repair.[9] As conditions that mimic those present in the intervertebral disc have been shown to promote MSC differentiation into disc-like cells,[31] there is also the possibility that reversine can be used to generate cells expressing the annulus fibrosus characteristics. In this case, it may be possible to utilize epigenetic reprogramming to replace or repair each of the major tissues of the disc. Of course, from the stand point of regenerative therapy, as the annulus fibrosus cells would be harvested from a degenerated disc and may not be normal, the response to reversine treatment would likely be different from those utilized in this study. Work is in progress to characterize responses of annulus fibrosus cells isolated from degenerated disc to reversine and to define environmental conditions that exist within the different compartments of disc, which might enhance reversine-dependent differentiation of progenitor-like cells into defined lineages.

Acknowledgment

This study was funded by NIH (R01AR050087 and R01AR055655).

Disclosure Statement

None of the authors have any conflict of interest in connection with this article.

References

1. Risbud, M.V., Shapiro, I.M., Vaccaro, A.R., and Albert, T.J. Stem cell regeneration of the nucleus pulposus. Spine J **4**, 348S, 2004.
2. Roberts, S. Disc morphology in health and disease. Biochem Soc Trans **30**, 864, 2002.
3. Sakai, D., Mochida, J., Iwashina, T., Hiyama, A., Omi, H., Imai, M., Nakai, T., Ando, K., and Hotta, T. Regenerative effects of transplanting mesenchymal stem cells embedded in atelocollagen to the degenerated intervertebral disc. Biomaterials **27**, 335, 2006.
4. Sakai, D., Mochida, J., Yamamoto, Y., Nomura, T., Okuma, M., Nishimura, K., Nakai, T., Ando, K., and Hotta, T. Transplantation of mesenchymal stem cells embedded in atelocollagen gel to the intervertebral disc: a potential therapeutic model for disc degeneration. Biomaterials **24**, 3531, 2003.
5. Ganey, T., Libera, J., Moos, V., Alasevic, O., Fritsch, K.G., Meisel, H.J., and Hutton, W.C. Disc chondrocyte transplantation in a canine model: a treatment for degenerated or damaged intervertebral disc. Spine **28**, 2609, 2003.
6. Gruber, H.E., Johnson, T.L., Leslie, K., Ingram, J.A., Martin, D., Hoelscher, G., Banks, D., Phieffer, L., Coldham, G., and Hanley, E.N., Jr. Autologous intervertebral disc cell implantation: a model using *Psammomys obesus*, the sand rat. Spine **27**, 1626, 2002.
7. Sakai, D., Mochida, J., Iwashina, T., Watanabe, T., Nakai, T., Ando, K., and Hotta, T. Differentiation of mesenchymal stem cells transplanted to a rabbit degenerative disc model: potential and limitations for stem cell therapy in disc regeneration. Spine **30**, 2379, 2005.
8. Wuertz, K., Godburn, K., and Iatridis, J.C. MSC response to pH levels found in degenerating intervertebral discs. Biochem Biophys Res Commun **379**, 824, 2009.
9. Sakai, D. Future perspectives of cell-based therapy for intervertebral disc disease. Eur Spine J **17 Suppl 4**, 452, 2008.
10. Risbud, M.V., Guttapalli, A., Tsai, T.T., Lee, J.Y., Danielson, K.G., Vaccaro, A.R., Albert, T.J., Gazit, Z., Gazit, D., and Shapiro, I.M. Evidence for skeletal progenitor cells in the degenerate human intervertebral disc. Spine **32**, 2537, 2007.
11. Chen, S., Zhang, Q., Wu, X., Schultz, P.G., and Ding, S. Dedifferentiation of lineage-committed cells by a small molecule. J Am Chem Soc **126**, 410, 2004.
12. Anastasia, L., Sampaolesi, M., Papini, N., Oleari, D., Lamorte, G., Tringali, C., Monti, E., Galli, D., Tettamanti, G., Cossu, G., and Venerando, B. Reversine-treated fibroblasts acquire myogenic competence *in vitro* and in regenerating skeletal muscle. Cell Death Differ **13**, 2042, 2006.
13. Igura, K., Zhang, X., Takahashi, K., Mitsuru, A., Yamaguchi, S., and Takashi, T.A. Isolation and characterization of mesenchymal progenitor cells from chorionic villi of human placenta. Cytotherapy **6**, 543, 2004.
14. Risbud, M.V., Fertala, J., Vresilovic, E.J., Albert, T.J., and Shapiro, I.M. Nucleus pulposus cells upregulate PI3K/Akt and MEK/ERK signaling pathways under hypoxic conditions and resist apoptosis induced by serum withdrawal. Spine **30**, 882, 2005.
15. Jaiswal, N., Haynesworth, S.E., Caplan, A.I., and Bruder, S.P. Osteogenic differentiation of purified, culture-expanded human mesenchymal stem cells *in vitro*. J Cell Biochem **64**, 295, 1997.
16. Pittenger, M.F., Mackay, A.M., Beck, S.C., Jaiswal, R.K., Douglas, R., Mosca, J.D., Moorman, M.A., Simonetti, D.W., Craig, S., and Marshak, D.R. Multilineage potential of adult human mesenchymal stem cells. Science **284**, 143, 1999.
17. Janderová, L., McNeil, M., Murrell, A.N., Mynatt, R.L., and Smith, S.R. Human mesenchymal stem cells as an *in vitro* model for human adipogenesis. Obes Res **11**, 65, 2003.
18. Amabile, G., D'Alise, A.M., Iovino, M., Jones, P., Santaguida, S., Musacchio, A., Taylor, S., and Cortese, R. The Aurora B kinase activity is required for the maintenance of the differentiated state of murine myoblasts. Cell Death Differ **16**, 321, 2009.
19. Musacchio, A., and Salmon, E.D. The spindle-assembly checkpoint in space and time. Nat Rev Mol Cell Biol **8**, 379, 2007.
20. Sabbattini, P., Canzonetta, C., Sjoberg, M., Nikic, S., Georgiou, A., Kemball-Cook, G., Auner, H.W., and Dillon, N. A novel role for the Aurora B kinase in epigenetic marking of

silent chromatin in differentiated postmitotic cells. EMBO J 26, 4657, 2007.
21. Stadtfeld, M., Maherali, N., Breault, D.T., and Hochedlinger, K. Defining molecular cornerstones during fibroblast to iPS cell reprogramming in mouse. Cell Stem Cell 2, 230, 2008.
22. Yu, J., Hu, K., Smuga-Otto, K., Tian, S., Stewart, R., Slukvin, I.I., and Thomson, J.A. Human induced pluripotent stem cells free of vector and transgene sequences. Science 324, 797, 2009.
23. Chen, S., Takanashi, S., Zhang, Q., Xiong, W., Zhu, S., Peters, E.C., Ding, S., and Schultz, P.G. Reversine increases the plasticity of lineage-committed mammalian cells. Proc Natl Acad Sci USA 104,10482, 2007.
24. Shan, S.W., Tang, M.K., Chow, P.H., Maroto, M., Cai, D.Q., and Lee, K.K. Induction of growth arrest and polycomb gene expression by reversine allows C2C12 cells to be reprogrammed to various differentiated cell types. Proteomics 7, 4303, 2007.
25. Kim, Y.K., Choi, H.Y., Kim, N.H., Lee, W., Seo, D.W., Kang, D.W., Lee, H.Y., Han, J.W., Park, S.W., and Kim, S.N. Reversine stimulates adipocyte differentiation and down-regulates Akt and p70(s6k) signaling pathways in 3T3-L1 cells. Biochem Biophys Res Commun 358, 553, 2007.
26. Van Overstraeten-Schlögel, N., Beguin, Y., and Gothot, A. Role of stromal-derived factor-1 in the hematopoietic-supporting activity of human mesenchymal stem cells. Eur J Haematol 76, 488, 2006.
27. Djouad, F., Charbonnier, L.M., Bouffi, C., Louis-Plence, P., Bony, C., Apparailly, F., Cantos, C., Jorgensen, C., and Noël, D. Mesenchymal stem cells inhibit the differentiation of dendritic cells through an interleukin-6-dependent mechanism. Stem Cells 25, 2025, 2007.
28. Rafani, C., Luchetti, L., Testa, G., Lasorella, R., Isacchi, G., Bottazzo, G.F., and Berardi, A.C. IL-16 can synergize with early acting cytokines to expand *ex vivo* CD34+ isolated from cord blood. Stem Cells Dev 18, 671, 2009.
29. Pevsner-Fischer, M., Morad, V., Cohen-Stady, M., Rousso-Noori, L., Zanin-Zhorov, A., Cohen, S., Cohen, I.R., and Zipori, D. Toll-like receptors and their ligands control mesenchymal stem cell functions. Blood 109, 1422, 2007.
30. Opitz, C.A., Litzenburger, U.M., Lutz, C., Lanz, T.V., Tritschler, I., Köppel, A., Tolosa, E., Hoberg, M., Anderl, J., Aicher, W.K., Weller, M., Wick, W., and Platten, M. Toll-like receptor engagement enhances the immunosuppressive properties of human bone marrow-derived mesenchymal stem cells by inducing indoleamine-2,3-dioxygenase-1 via interferon-beta and protein kinase R. Stem Cells 27, 909, 2009.
31. Risbud, M.V., Albert, T.J., Guttapalli, A., Vresilovic, E.J., Hilibrand, A.S., Vaccaro, A.R., and Shapiro, I.M. Differentiation of mesenchymal stem cells towards a nucleus pulposus-like phenotype *in vitro*: implications for cell-based transplantation therapy. Spine 29, 2627, 2004.

Address correspondence to:
Makarand V. Risbud, Ph.D.
Department of Orthopaedic Surgery and Graduate Program in Tissue Engineering and Regenerative Medicine
Thomas Jefferson University
Suite 501 Curtis Bldg.
1015 Walnut St.
Philadelphia, PA 19107

E-mail: makarand.risbud@jefferson.edu

Received: May 22, 2009
Accepted: November 24, 2009
Online Publication Date: February 1, 2010